

# **Dip Sequence Analysis Utilizing Statistical Curvature Analysis: A Case Study on Complex Strata of the Late Middle Miocene Formation in Akita Basin, Onshore Japan\***

**Sarvagya Parashar<sup>1</sup>, Ivan Zhia Ming Wu<sup>1</sup>, Saki Shimada<sup>2</sup>, Hideo Komatsu<sup>2</sup>, M.S Iyer<sup>1</sup>, and Lee Chung Yee<sup>1</sup>**

Search and Discovery Article #42346 (2019)\*\*

Posted January 14, 2019

\*Adapted from extended abstract prepared in conjunction with oral presentation given at 2018 International Conference and Exhibition, Cape Town, South Africa, November 4-7, 2018

\*\*Datapages © 2019 Serial rights given by author. For all other rights contact author directly. DOI:10.1306/42346Parashar2019

<sup>1</sup>FRS, Halliburton Energy Services, Kuala Lumpur, Malaysia ([Ivanzhiaming.wu@halliburton.com](mailto:Ivanzhiaming.wu@halliburton.com))

<sup>2</sup>Inpex Corporation, Akita, Japan

## **Abstract**

The variation of dips from point to point in the subsurface is related to the bulk curvature of the structural setting. Conventionally, consistent shale bedding dips or low magnitude consistent bedding are selected and filtered out to interpret only the transverse section of the wellbore and to define the subsurface dip sequences obtained from the microresistivity images or dipmeter data. In this study, lithological complexity and its associated structures create uncertainty in shale identification, making it difficult to analyze the structural dip pattern.

Zone 1 shows a consistent average dipping azimuth toward the east, with increasing dip magnitude from the top to base. Zone 2 exhibits the same azimuth, however, with the dip magnitude decreasing from approximately 70 degrees to less than 10 degrees. The most significant change occurs in Zone 3 where the dipping orientation changed dramatically. The dip-azimuth plot revealed the trends of beddings, primarily toward the south at the lower part and dipping toward the east toward the upper part. The dip trends in the longitudinal dip component plot with depth in the study well exhibit considerable scatter that may be attributable to the steep dips zone. The transverse dip component exhibits the distinctive negative cusp pattern. The dips exhibit the downward increase in magnitude until they reach the drag zone, then return to the normal dip magnitude trend. In the present well, the dips increase from 10 degrees to approximately 70 degrees and are greater between the trough and crestal plane areas. The statistical curvature analysis technique (SCAT) analysis detected the presence of a subseismic plunging normal fault crossing the drilled section. This normal fault has a flattening drag that plunges at 8 degrees across the longitudinal direction of approximately 160 degrees (strike).

This model may be used for the constraints of structural interpretation where seismic data is inconclusive. It was beneficial in revealing subsurface structural geometry. This model helps to decipher the subseismic structural geometry of the target structure in high resolution, provide more detailed structural information, and visualize possible different structural zonations in the drilled section.

## Introduction

This paper describes the statistical curvature analysis technique (SCAT), which has been proven to be useful for the structural interpretation of dips sequence data acquired from the microresistivity images tools. The SCAT technique is based on four empirical verified geometrical concepts known as structural bulk curvature, transverse and longitudinal structural directions, structural surfaces and related dip profile special points, and dip isogons. SCAT actually resolves the data into two mutually perpendicular transverse and longitudinal components, which are subsequently plotted as a function of downhole depth. Generally, transverse direction is defined as the cross-sectional view through the well that exhibits the maximum structural changes, whereas the longitudinal direction represents the cross section that exhibits the minimum structural changes.

The bulk curvature can be assigned to one of the four general categories: planar, singly curved, plunge reversal, or domal bulk curvature. Transverse (T) and longitudinal (L) directions, along with structural bulk curvature, provides the capability of obtaining the true structural dips from the analysis of dip sequences. They also provide the means for calculating the bearing and plunge of the crestal and trough lines of folds, finding strike and dips of crestal, axial, and inflection planes of the folds, and the strike and dip direction of dip-slip faults (Bengtson, 1981).

The area of the present study is located in the Yabase Oil Field in the central provenance of the Akita Basin in Japan. Yabase is the largest oil field in Japan; its cumulative production through the end of 1979 was 5.1 million kl of crude oil and 1100 million m<sup>3</sup> of natural gas. The total annual production reached a maximum of 0.3 million kl of oil in 1959 and thereafter gradually decreased to 0.02 million kl by 1979 (Aoyagi and Iijima, 1983). The trap is a north-south elongated, symmetrical anticline that parallels the regional strike. The structure is approximately 15 km long from north to south and 0.5 km wide from east to west (Aoyagi and Iijima, 1983). The primary reservoirs in the Yabase Oil Field range from the middle part of the Miocene Onnagawa Formation to the upper part of the Pliocene Lower Tentokuji Formation ([Figure 1](#)).

The present well was drilled to evaluate the low permeability reservoir in the area north of the Yabase Oil Field; this area is known for its low permeability and low flow characteristics. [Figure 2](#) shows a generalized stratigraphy column of the Yabase Oil Field.

## Methodology

The detailed evaluation of the microresistivity image was performed in the 8.5-in. section of well X in the Yabase Oil Field. During a thorough examination on the image features, a total of 1,828 dips were picked and classified manually to define the structural and sedimentological feature in the logged interval. The typical shale section in the entire logged interval is not evident; consequently, the overall structural dip was not computed based on the shale bedding dip magnitude. During a detailed dip pattern analysis, the variation in the dip magnitude and their azimuthal reversal is exhibited. Typically, three major dip patterns are evident in the entire logged interval; from top to the bottom, the dip magnitude continuously exhibits an increase in magnitude toward the east-southeast. The middle portion exhibits relatively high dip magnitudes, as compared to the top section, which displays the typical dip drag pattern usually associated with the normal growth fault or attributable to any other structural discontinuity. This trend is followed by the sudden azimuthal reversal of the dips toward the south-southwest with a mean dip magnitude of 22.4 degrees. However, the statistical average of bed boundaries associated with volcanic sedimentary section (interval) exhibits a mean dip of 21.8 degrees toward the east-southeast.

Because the typical shale section is not evident in the drilled section, a SCAT analysis was adopted to decipher the overall true structural dip and associated structural pattern or zones. A total of six different planar features were defined in this study. These features are represented by various sets of colored symbols and tadpoles that are summarized in [Figure 3](#). The quality of the dip pick was assessed computationally by the programs or assigned manually by the image analyst. In either case, the quality can be identified by the fill inside the head of the tadpole. [Figure 4](#) shows the five quality levels used.

Further analysis of the beddings and bandings dips statistics provided interesting observations in the logged interval. Throughout the interval, the demarcations of three zones are well evident, based on the trends of the dips that were picked. From [Figure 5](#), the upper interval, denoted by Zone 1 (red), shows a consistent average dipping azimuth toward the east with an increasing dip magnitude across an interval of approximately 200 m. In Zone 2 (blue), the azimuth still exhibits an average eastward direction, however, with the dip showing a decreasing magnitude from approximately 70 degrees to less than 10 degrees. The more significant change is evident in Zone 3 (yellow) in which both the dipping magnitude and azimuth change dramatically. The dip-azimuth plot revealed the trends of beddings, primarily toward the south to south-southwest at the lower part of Zone 3 and dipping to the east toward the upper part represented by Zones 1 and 2 ([Figure 5](#)). There is no clear shale interval that can be used to refine a better control on the structure that may or may not contribute to this dip orientation. Based on these observations, a structural discontinuity may be present between these zones (represented by the two red horizontal lines in [Figure 5](#)) because this is a clear, evident change in the dip orientations.

## Results

The variation of dips from point to point in the subsurface and the variation in the angle are related to the bulk curvature of the structural setting. The bulk curvature and related transverse and longitudinal structure directions of any well setting can usually be determined by SCAT. The bulk curvature is based upon the analysis of dip magnitude with respect to depth, azimuthal reversal with respect to depth, amount of dip magnitude with respect azimuth, transverse dips component plot with depth, and longitudinal component with depth.

The longitudinal dip component vs. depth plots show the lower and less variable dip rather than the dip-component plot for any direction. The average L-direction component of the dip is zero for the planar and non-plunging fold settings and is equal to the angle of the plunge for plunging fold settings. The dip trends in the longitudinal dip component plot with depth in the studied well exhibit considerable scatter that may attribute to steep dip zones.

The transverse dip component exhibits the distinctive cusp pattern, which makes it different from other possible structural patterns ([Figure 6](#)). From the local transverse dip component plot, it is evident from bottom to top that the relative dip azimuth is changing and moves toward the negative and then deflects back to the zero. This characteristic pattern is known as a negative cusp. The top deflection from zero toward the negative defines the trough plane (TP), whereas the reversal of the azimuth (track 2 in [Figure 6](#)) marks the crestal plane (CP).

The dip vs. depth plot exhibits an almost mirror image of transverse dip component plot. Moving from the top to bottom, the dip exhibits the downward increase in magnitude until it reaches the drag zone, then returns to the normal dip magnitude trend. In the present well, the dips show an increase from 10 degrees to approximately 70 degrees, with the highest value between the TP and CP areas.

The azimuth vs. depth plot exhibits the sudden reversal of the dip pattern from Zone 2 to Zone 3, which remains consistent in Zone 3, with a slight increase in the dip magnitude. The dominant direction remains toward the south. A closer examination of the local longitudinal dip component plot shows that the drag effect is minimum in the longitudinal direction. Most of the scatter of the dip set lies between 0 to 30 degrees, with no deflection toward the adjacent quadrant. The SCAT analysis results suggest that the well encountered the normal fault with a flattening drag, with a plunge of 8-degree magnitude, across the longitudinal direction of 161 degrees (strike). The most probable analogous model for this regime is shown in [Figure 7](#) and [Figure 8](#).

### **Conclusions**

The case study presented describes the statistical curvature analysis technique for a structural interpretation of dip sequence data obtained from microresistivity image data acquired across the complex lithocolumn of volcanoclastic sequences. The volcanic sequence is highly heterogeneous; the complications increase with less evidence of the shale section for structural estimation, in which this technique is helpful. This technique plays an immense role in defining subseismic features and helps to build a reliable structural model of the formation. More often, it is possible to reconstruct the geometry of the geological structure and to derive high-resolution structural information from a dip-meter survey or the dip sequences obtained from microresistivity images, rather than only the dip along the wellbore.

### **Acknowledgement**

The authors express their sincere appreciation to Inpex Corporation management for permission to publish this study.

### **References Cited**

Aoyagi, K., and A. Iijima, 1983, Reservoir Characteristics and Petroleum Migration in the Miocene Onnagawa Formation of Akita, Japan, *in* C.M. Isaacs, R.E. Garrison, S.A. Graham, and W.A. Jensky II (eds.), *Petroleum Generation and Occurrence in the Miocene Monterey Formation, California, Pacific Section: Society of Economic Paleontologists and Mineralogists [now the Society for Sedimentary Geology]*, Los Angeles, California, May 20–22, 1983, Proceedings, p. 75–84.

Bengston, C.A., 1981, Statistical Curvature Analysis Technique for Structural Interpretation of Dipmeter Data: *American Association of Petroleum Geologists Bulletin*, v. 65/2, p. 312-332.

Sato, T., M. Yamasaki, and S. Chiyopnobu, 2009, *Geology of Akita Prefecture: Daichi*, v. 50, p. 70-83, (in Japanese).

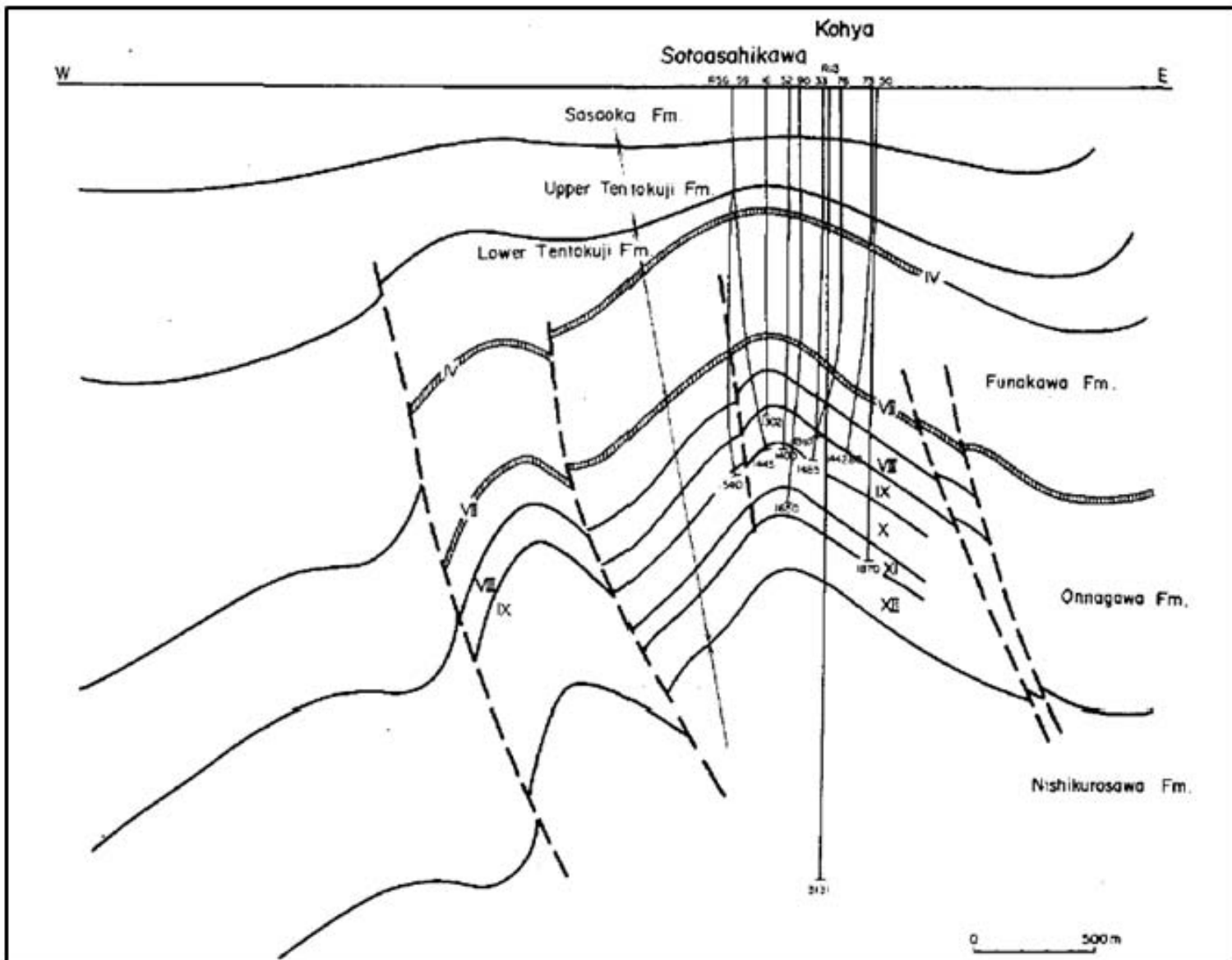


Figure 1. Geological cross section of Yabase Oil Field in Akita Basin, Japan (after Aoyagi and Iijima, 1983).

Yabase Field Standard Stratigraphy					
Age (Ma)			Formation	Reservoir	Lithology
1.81 2.75 3.85 5 13	Quaternary	Pleistocene	Marine sediments		Sandstone
			Terrace sediments		Mud/Sand/Gravel
	Neogene	Upper Pliocene	Sasaoka F.	I	Sandstone
			Tentokuji F.	II	Siltstone
			Katsurane F.	III	Alternation of Mudstone and Sandstone
		Lower Pliocene	Yabase tuff (Upper Nanakura tuff equivalent)	IV	Tuff
			Funakawa F.	V	Mudstone
				VI	Tuff
		Middle Miocene – Upper Miocene	(Lower Nanakura tuff equivalent)	VII	Tuff
			Onnagawa F.	VIII	Alternation of siliceous Mudstone and Tuff/Sandstone
			Aizen basalt	IX	Basalt
				X	
				XI	
				XII	
		Middle Miocene	Nishikurosawa F.		Mudstone
			?		?

\*Sato et al., 2009

Figure 2. Stratigraphic column of Yabase Field.




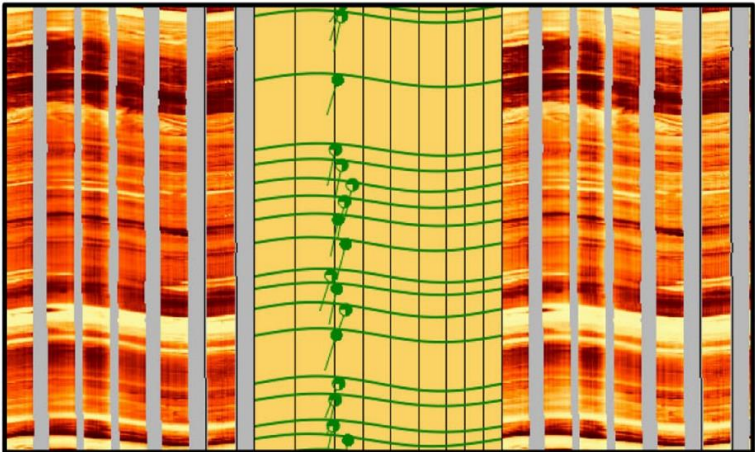

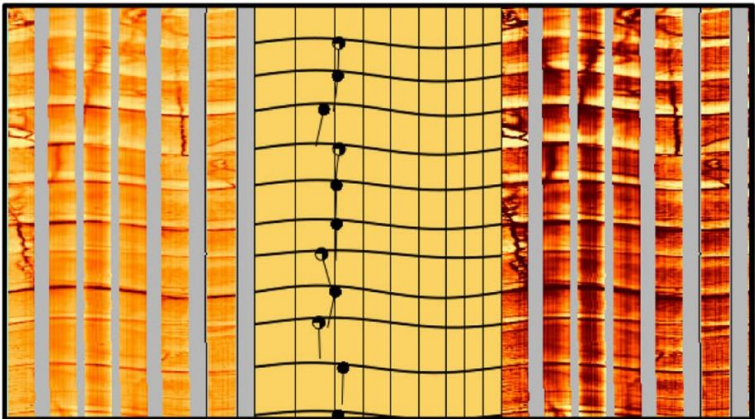

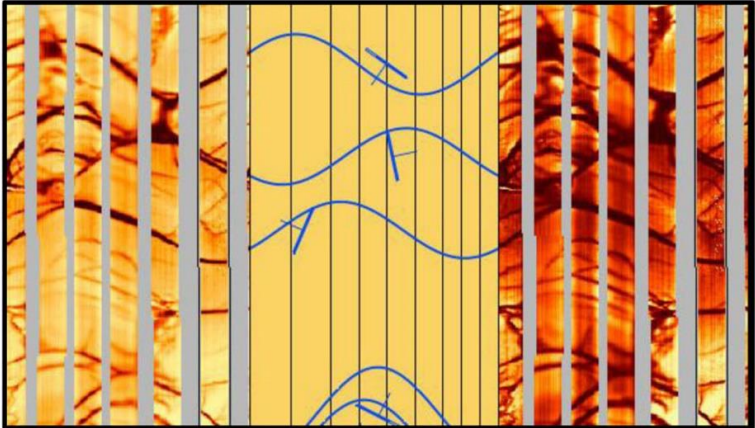

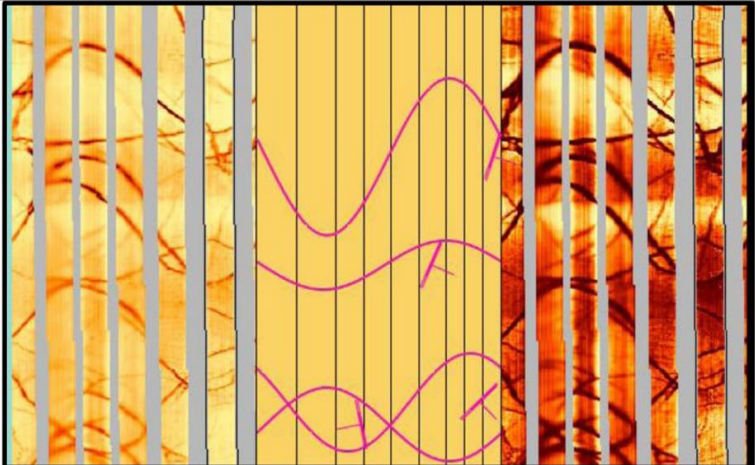

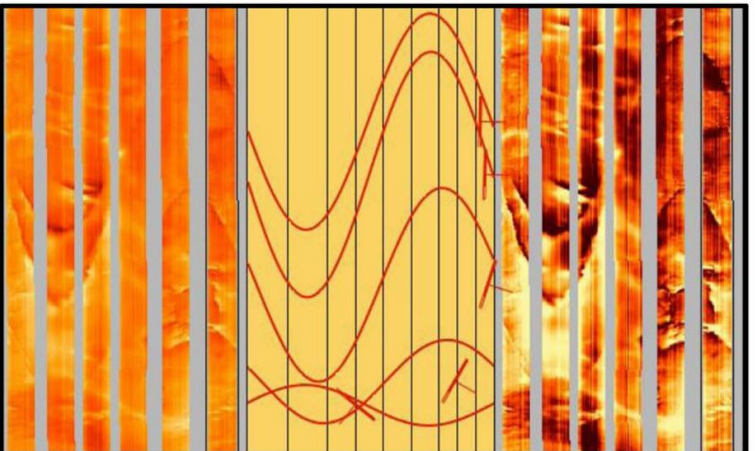

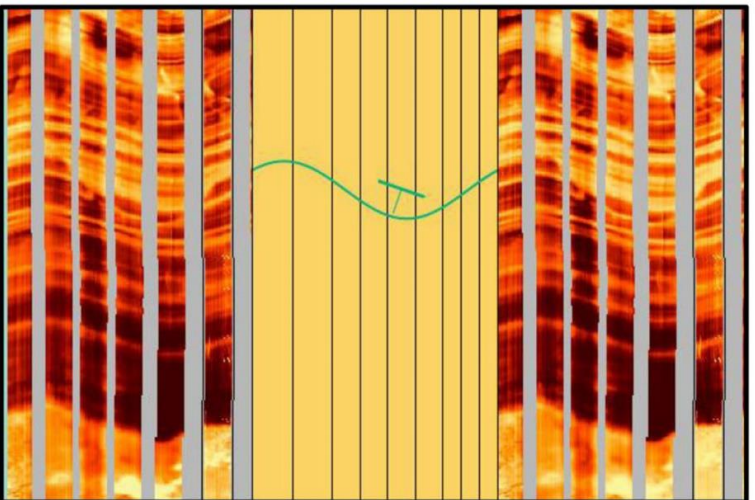
Plane type	Symbol and Color	Description	Image Examples
Beddings		Bedding features are parallel surfaces identified within tuffaceous or reworked sedimentary intervals. They may occasionally show deformation and indications of fluidal features.	
Banding		Banding features form consistent dip and azimuth. These are evident in resistive basaltic interval.	
Conductive/Open Fracture		Continuous planar features that appear to be electrically conductive or darker than surrounding rocks. Appears to be symmetrical, enabling a sine wave to be fit in them and can be mapped around the borehole.	
Partially healed/open Fracture		Discontinuous fractures that appear to be at least partially closed or mineralized. May appear as partially bright and partially dark traces and they are usually symmetrical.	
Healed/Closed Fracture		Continuous planar features that appear to be electrically resistive or brighter than surrounding rocks. Appears to be symmetrical enabling a sine wave to fit in them and can be traced around the borehole.	
Microfault		Display minor displacement in bedding along the fracture plane.	

Figure 3. Dip classification used in the study well.



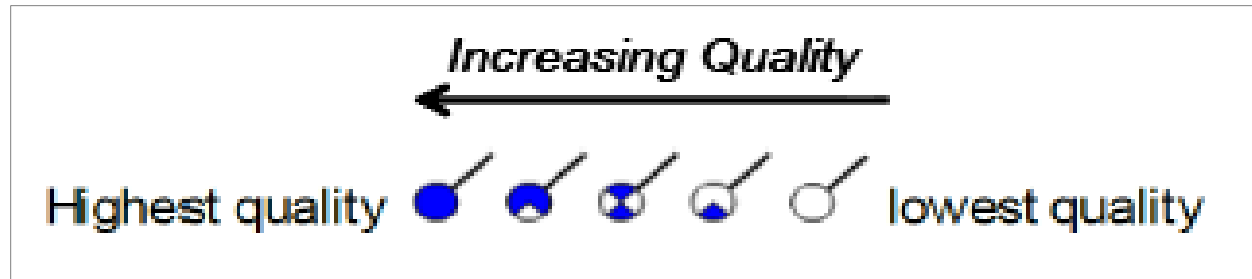


Figure 4. Five quality levels used in the study.

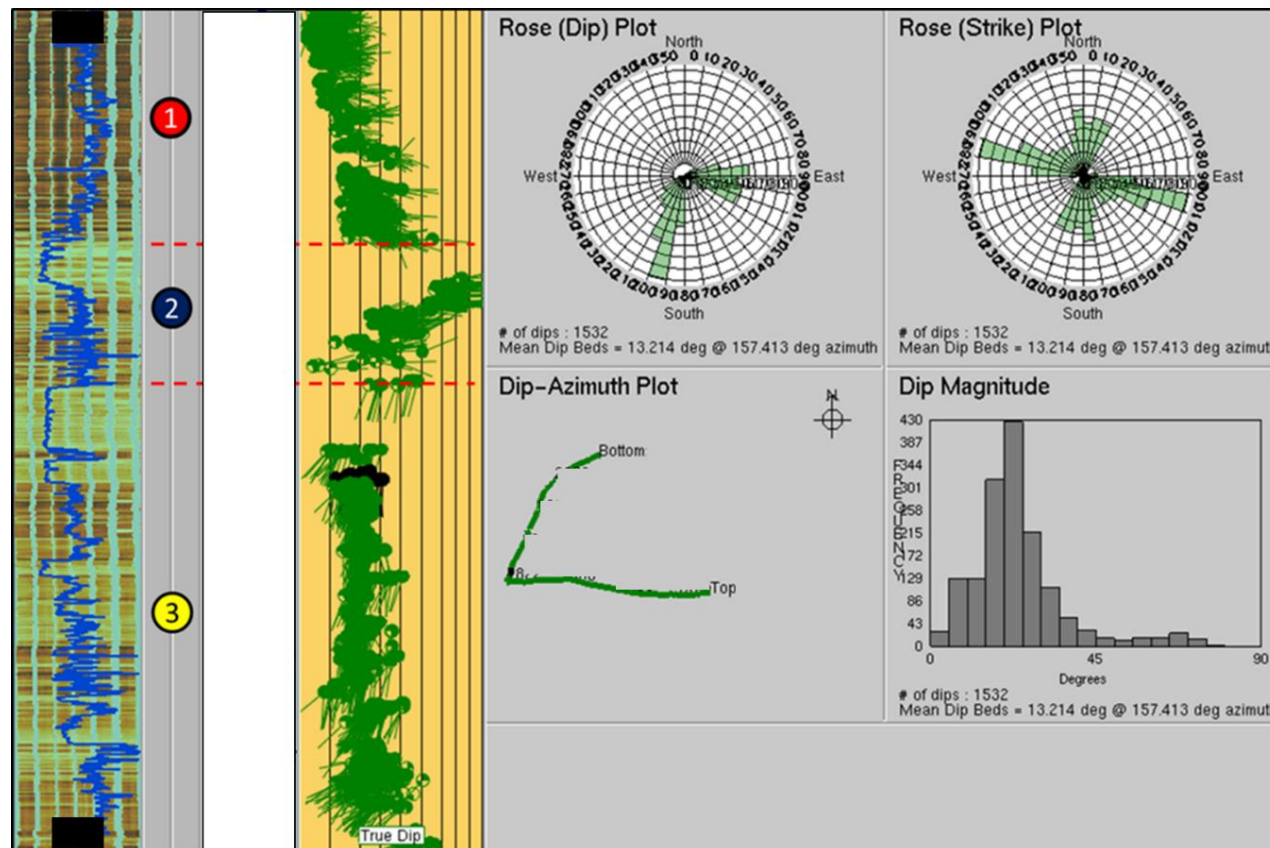


Figure 5. Rose plot (dip and strike), dip-azimuth plot, and dip magnitude histogram for beddings (green tadpole) and bandings (black tadpole) identified in the study interval.



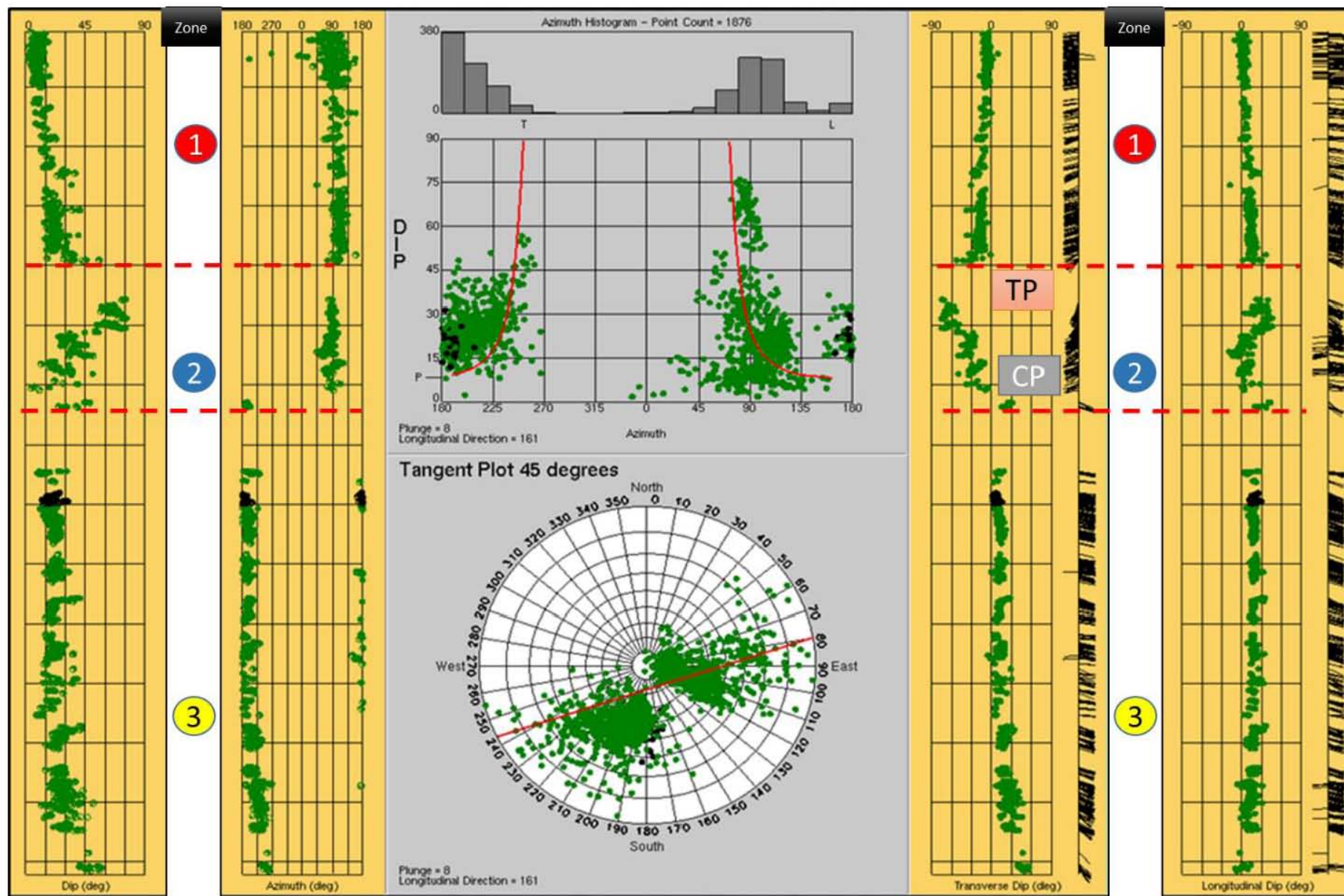


Figure 6. SCAT results of studied well across the 700 m drilled interval showing the dip and azimuth vs. depth on left track. The middle plot provides an azimuth histogram along with tangent plot. The right track shows the transverse dip and longitudinal dip vs. depth.

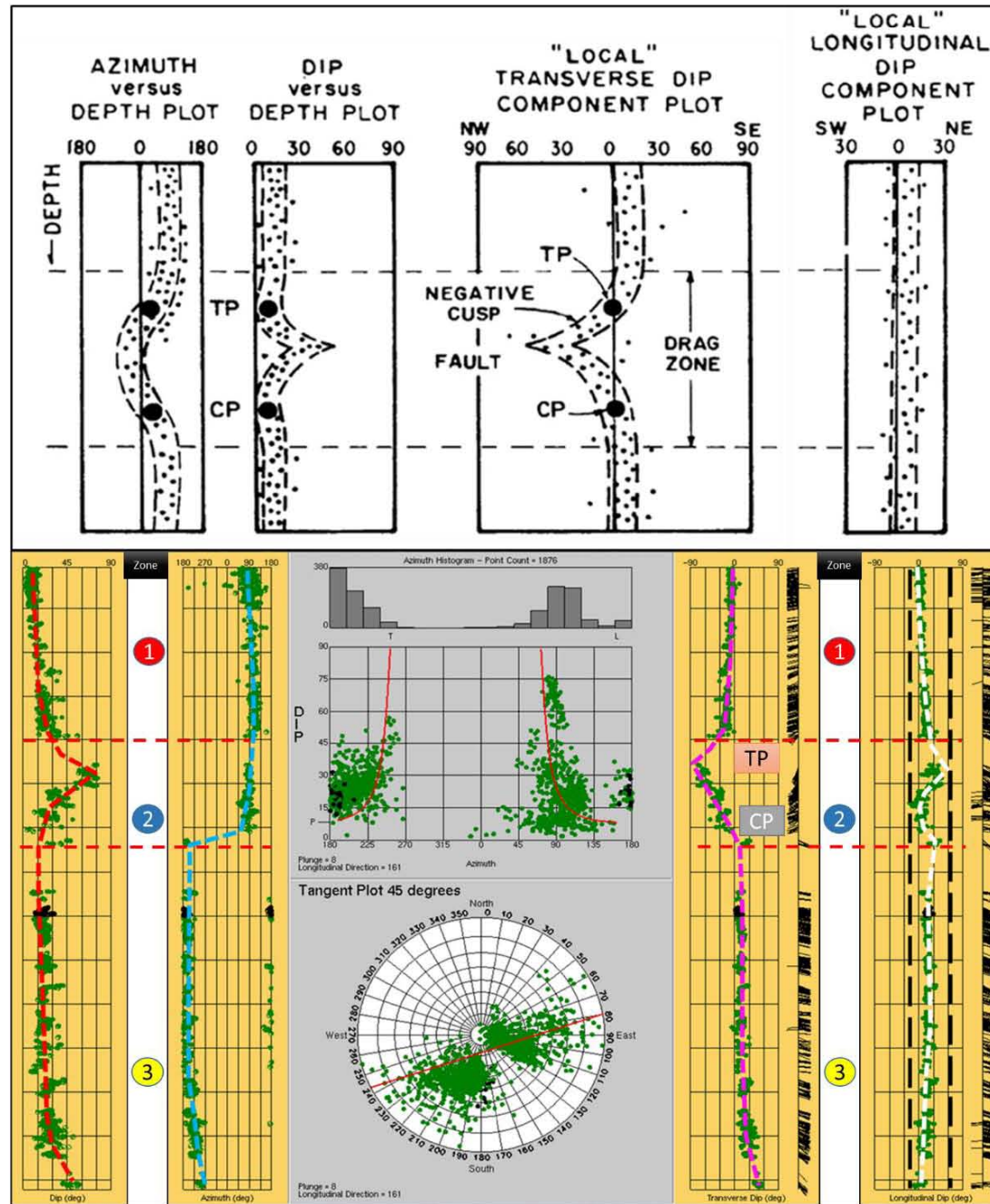


Figure 7. Top: SCAT model proposed by Bengston (1981) for normal fault with flattening and plunging drag. Below: Dip, azimuth, transverse dip, and longitudinal dip pattern recognition from study well.

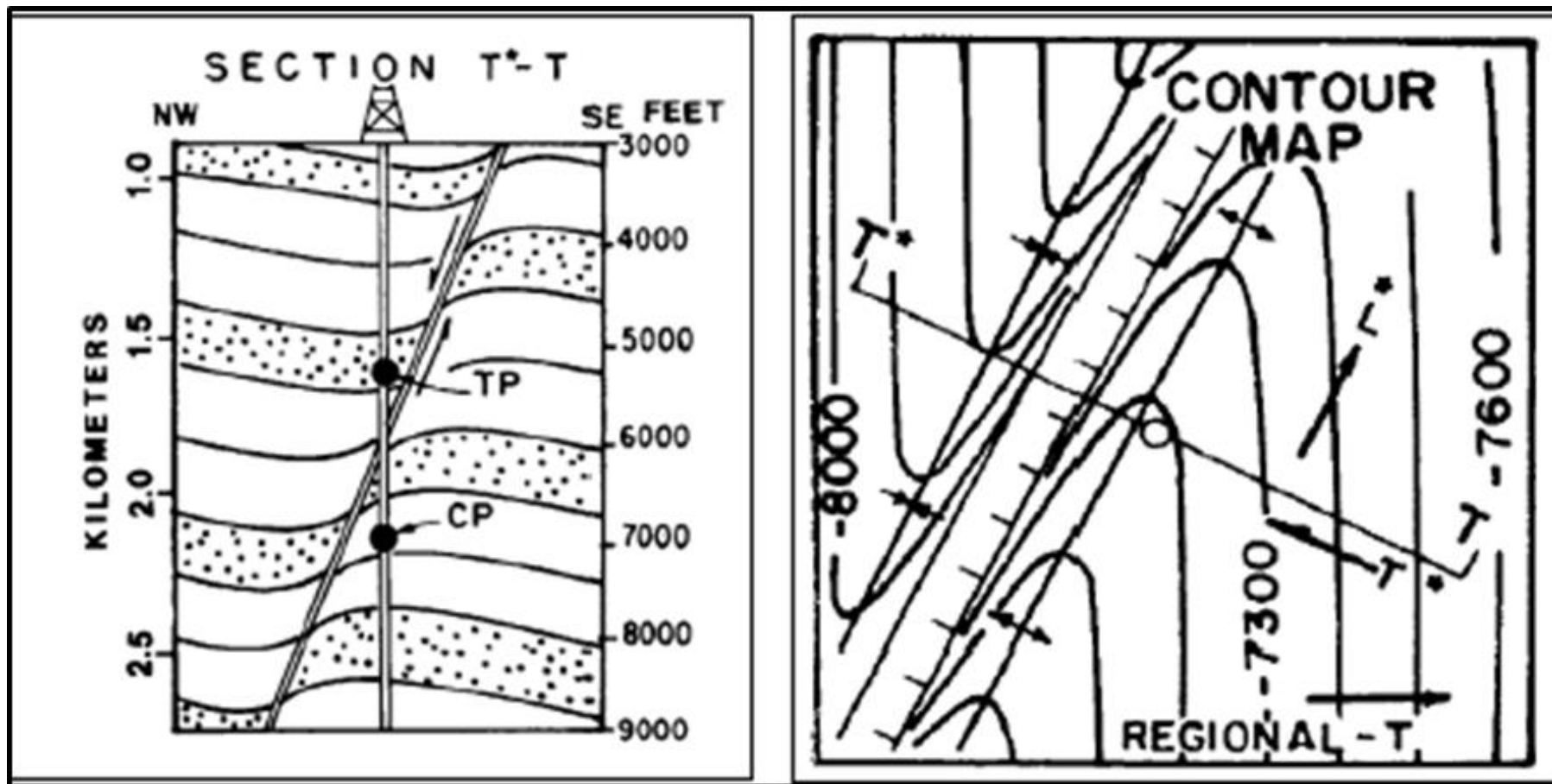


Figure 8. Structural model analogue representing the similar condition of study well, exhibiting a similar dip pattern encountered identified from SCAT analysis (Bengston, 1981).